

# A Small Molecule Smac Mimic Potentiates TRAIL- and TNF $\alpha$ -Mediated Cell Death

Lin Li,<sup>1\*</sup> Ranny Mathew Thomas,<sup>1\*</sup> Hidetaka Suzuki,<sup>1\*</sup>  
Jef K. De Brabander,<sup>1†</sup> Xiaodong Wang,<sup>1,2†</sup> Patrick G. Harran<sup>1†</sup>

We describe the synthesis and properties of a small molecule mimic of Smac, a pro-apoptotic protein that functions by relieving inhibitor-of-apoptosis protein (IAP)-mediated suppression of caspase activity. The compound binds to X chromosome-encoded IAP (XIAP), cellular IAP 1 (cIAP-1), and cellular IAP 2 (cIAP-2) and synergizes with both tumor necrosis factor  $\alpha$  (TNF $\alpha$ ) and TNF-related apoptosis-inducing ligand (TRAIL) to potently induce caspase activation and apoptosis in human cancer cells. The molecule has allowed a temporal, unbiased evaluation of the roles that IAP proteins play during signaling from TRAIL and TNF receptors. The compound is also a lead structure for the development of IAP antagonists potentially useful as therapy for cancer and inflammatory diseases.

Inhibitor-of-apoptosis proteins (IAPs) inhibit the enzymatic activity of caspases, cysteine proteases that execute the cell death program (1). IAPs bind directly to caspases with the use of a characteristic  $\sim$ 70-residue zinc-containing domain termed the baculovirus inhibitory repeat (Bir). Human X chromosome-encoded IAP (XIAP), cellular IAP 1 (cIAP-1), and cellular IAP 2 (cIAP-2) have three tandem repeats of the Bir domain in their N-terminal region, whereas other mammalian IAPs have a single Bir domain (2). XIAP is the most potent caspase inhibitor among IAPs, and it interacts with initiator caspase 9 and executioner caspases 3 and 7 through its Bir3 and Bir2 domains, respectively (3, 4). The role of cIAP 1 and 2 in apoptosis is less defined, although both are associated with the TNF $\alpha$  receptor 1 signaling complex (5, 6). XIAP potently inhibits activated caspases, those generated in situ from a corresponding zymogen after the stimulation of death receptors on the cell surface or after the release of pro-apoptotic factors from the intermembrane space of mitochondria into the cytosol (3). Because effector caspase activity is both necessary and sufficient for irrevocable programmed cell death, XIAP functions as a gatekeeper to this final stage of the process. IAP gene amplifications and protein overexpression have been found in many human cancers, suggesting a means by which these cells evade apoptosis during

tumorigenesis and become resistant to chemotherapy and radiation treatments (7–9).

IAP-mediated inhibition of apoptosis is countered by the second mitochondria-derived activator of caspases (Smac) (10, 11). Smac protein is secreted from mitochondria into the cytosol during apoptosis. There it interacts with Bir domains in IAPs with the use of four amino acid residues [AVPI (12)] at its N terminus (13, 14). Synthetic Smac N-terminal peptides fused to cell-permeabilizing peptides have been found to bypass mitochondrial regulation and sensitize both human cancer cells in culture and tumor xenografts in mice to apoptosis when combined with TNF-related apoptosis-inducing ligand (TRAIL) or chemotherapeutic drug treatments (15–18). Here, we describe a small molecule that functions similarly at  $10^5$ - to  $10^6$ -fold lower concentrations. The compound penetrates cell membranes and binds XIAP with an affinity equal to that of Smac itself. Moreover, as a true Smac mimetic, the molecule also binds and eliminates cIAP-1 and cIAP-2 activities and promotes both TRAIL- and TNF $\alpha$ -induced apoptosis at low nanomolar concentrations in cancer cell culture.

The co-crystal structure of Smac in complex with the XIAP Bir3 domain shows the Smac N terminus interacts with a groove formed on the Bir3 surface (13). The four Smac residues (AVPI) that contact Bir3 do so by docking a fourth strand onto an existent three-stranded antiparallel  $\beta$  sheet. Structural variations in the C-terminal end of the tetrapeptide are tolerated, and AVPF (12) actually outperforms AVPI as a Smac mimetic in vitro. We therefore used computer-simulated conformations of AVPF as a guide to design nonpeptidyl replacements for its C-terminal half (PF). Each was synthesized in optically active form, immobilized onto the surface of polystyrene beads, and used to generate a set of compounds having variable amino

acids at position two and L-alanine at position one (19). The resultant hybrid mimetics (180 compounds) were released from solid support, purified, and evaluated for their ability to compete at the Smac binding site on recombinant XIAP-Bir3 (14). In this format, oxazoline 1 was the most potent competitor (Fig. 1, A and B). However, a number of its relatives had comparable affinity for the Bir3 domain, and no compound performed better than AVPF. When 1 was tested for stimulation of deoxyadenosine triphosphate (dATP)-dependent caspase 3 activation in soluble HeLa extracts, its potency exceeded that of synthetic AVPF but was orders of magnitude less than recombinant Smac. This troubling situation remained unchanged until modifications of 1 reached tetrazoyl thioethers of type 2. Attempts at a particular manipulation of the alkyne in 2 produced a by-product eventually characterized as C<sub>2</sub>-symmetric diyne 3, the endpoint of an oxidative homodimerization known as a Glaser coupling (20). Dimer 3 and its corresponding monomer 2 have comparable affinity for an isolated XIAP Bir3 domain (Fig. 1B). However, in a caspase 3 activation assay that measures neutralization of endogenous IAP activity in HeLa cell extract, diyne 3 is much more active as a Smac mimetic (Fig. 1D). The reason for this large discrepancy is likely attributable to bivalency. In particular, that compound 3 may interact simultaneously with adjacent Bir domains in XIAP. The resultant two-point bound complex may be considerably more stable than single-site affinities would predict (21). Recent evidence suggests that Smac, a native homodimer, binds XIAP similarly (22).

Complexes of Smac and full-length XIAP can be visualized by Coomassie Blue staining after nondenaturing gel electrophoresis. Incubation of XIAP with Smac (1:1.6 molar ratio) produces a high molecular weight complex that is completely disrupted by inclusion of a twofold molar excess of compound 3 (Fig. 1C). In fact, equal molar amounts of 3 disrupt more than half of the XIAP/Smac complex (lane 8). To the extent that equilibrium is reached under these conditions, the data suggest that compound 3 has a higher affinity for XIAP than does Smac. The latter interaction has  $K_D \sim 300$  pM when measured with full-length Smac and a Bir2+Bir3-containing segment of XIAP (22). Monomer 2 and control 4 (both alanine residues carbamoylated) have no effect on the Smac/XIAP complex, even when present in fivefold excess (lanes 11 and 13). Like Smac, compound 3 also competitively blocks the interaction of XIAP with active caspase 9 in vitro (Fig. 1F) (23).

To test the activity of compound 3 in vivo, we added it in varying amounts to T98G cells. T98G is a human glioblastoma cell line resistant to DNA damage-induced apoptosis. Compound 3 alone at high concentrations ( $>1$   $\mu$ M) does not induce apoptosis (Fig. 2A) or caspase 8 activation (Fig. 2B). However,

<sup>1</sup>Department of Biochemistry and <sup>2</sup>Howard Hughes Medical Institute, University of Texas Southwestern Medical Center at Dallas, 5323 Harry Hines Boulevard, Dallas, TX 75390–9038, USA.

\*These authors contributed equally to the work.

†To whom correspondence should be addressed. E-mail: pharra@biochem.swmed.edu (P.G.H.), xwang@biochem.swmed.edu (X.W.), jdebra@biochem.swmed.edu (J.K.D.)

## REPORTS

when used in combination with TRAIL (50 ng/mL), 100 nM of **3** causes extensive cell death (Fig. 2A). In fact, caspase 8 activation and apoptosis are observed at concentrations of **3** as low as 100 pM when combined with 50 ng/mL TRAIL (Fig. 2B). TRAIL alone at 50 ng/mL induces neither caspase 8 activation nor apoptosis in this cell line. Down-

stream caspase 3 activity in response to **3** plus TRAIL was monitored by Western blot analysis of cleaved poly(adenosine diphosphate-ribose)polymerase (PARP), a caspase 3 substrate (Fig. 2B). Endogenous PARP begins to be cleaved in the presence of 30 pM of **3** and 50 ng/mL TRAIL (lane 10, fig. S3). Control compound **4** has no effect in this assay. Importantly,

unlike the situation in cancer cells, compound **3** alone (10  $\mu$ M) or in combination with TRAIL had no detectable effects on primary cultures of human skin fibroblasts (23).

To verify that dimer **3** targets IAPs in cells, we synthesized a biotinylated variant. Although the display and spacing of monomers within this construct differs slightly

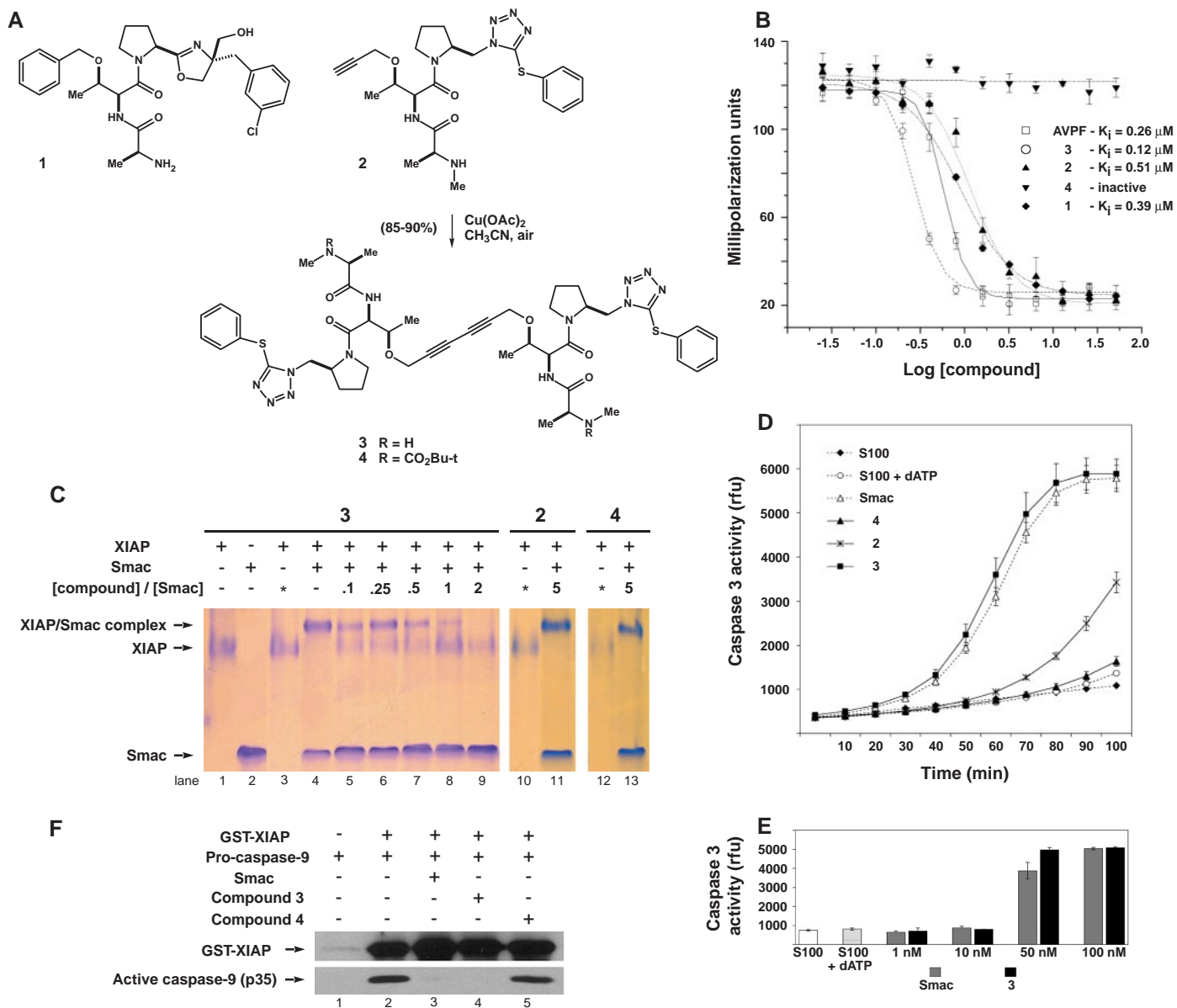


**Fig. 1.**  $C_2$ -symmetric compound **3** is a potent Smac mimetic in vitro. (A) Chemical structures of the small molecules described in this study. (B) Fluorescence polarization assay for the interaction of Smac and mimetics with the Bir3 domain of human XIAP. A synthetic Smac peptide [AVPIAQKSEK (12)] was C-terminally labeled with Alexafluor488 (Molecular Probes), and its complex with recombinant XIAP Bir3 (residues 241 to 356) was used to evaluate competitive Bir3 domain binding by synthetic small molecules (74). (C) Polyacrylamide gel electrophoresis under non-denaturing conditions and Coomassie Blue staining were used to evaluate the binding of **3** to recombinant full-length human XIAP. XIAP (5  $\mu$ M) and Smac (8  $\mu$ M) were incubated for 30 min at 37°C with or without prior treatment with varying amounts of **3**. Asterisks indicate that compound alone (40  $\mu$ M) was present along with XIAP in lanes 3, 10, and 12. (D) Time course comparison of caspase 3 activation by recombinant Smac

and small molecule mimetics. HeLa S100 was activated with 1 mM dATP. Either Smac (100 nM) or a small molecule (100 nM) was then added. The onset of caspase 3 activity was monitored as a fluorogenic substrate (Ac-DEVD-AMC, CalBiochem) was cleaved in situ, relative fluorescence units). (E) Bar graph representation of the same experiment performed in (D) except with varying concentrations of Smac and compound **3**. (F) Smac and compound **3** compete with glutathione S-transferase (GST)-tagged human XIAP for active caspase 9 binding. Pro-caspase 9 (0.9  $\mu$ M) was activated with 20 nM Apaf-1, 100 nM cytochrome C, and 1 mM dATP and then incubated with recombinant GST-XIAP for 3 hours at 30°C either in the absence (lane 2) or presence (lane 3) of Smac (1  $\mu$ M), compound **3** (1  $\mu$ M, lane 4), or compound **4** (1  $\mu$ M, lane 5). Western blots for active caspase 9 that subsequently associates with added glutathione-coated beads are shown.

from compound **3**, the molecule functions equally well to relieve IAP inhibition of caspase 3 in HeLa cell extracts (fig. S2). When biotinylated **3** was added to T98G cell extracts and recovered with streptavidin-coated beads, Western blots of associated proteins showed the presence of XIAP, cIAP-1, and cIAP-2 (Fig. 2C). Preincubating T98G cells with excess **3** blocked these affinity purifications, and a biotinylated control had no detectable IAP affinity in this format. These results suggest that compound **3** facilitates TRAIL-induced apoptosis by neutralizing the effects of multi-Bir domain-containing IAPs.

Related observations have been made

with the use of Smac peptides. However, these experiments focused on XIAP as a mediator of their effects (15–18). The finding that **3** binds to cIAP 1 and 2 suggested the additional opportunity to probe the role of these proteins in TNF $\alpha$  signaling. Both are present in TNF $\alpha$  receptor-1 signaling complexes (5, 6), but whether they inhibit caspase 8 or promote nuclear factor  $\kappa$ B (NF- $\kappa$ B) and c-Jun N-terminal kinase (JNK) signaling (24), or both, was not clear. Treatment of HeLa cells with compound **3** (100 nM) in combination with TNF $\alpha$  causes extensive apoptosis (Fig. 3A). Caspase 8 activation was observed within 2 hours (Fig. 3C), and cleavage of endogenous PARP, indicative of

caspase 3 activity, was detected after 4 hours. The effect of compound **3** in this case was comparable to that of 10  $\mu$ M cycloheximide (Fig. 3B). TNF $\alpha$  treatment, either alone or in combination with monomer **2** or control compound **4** (Fig. 3A), had no such effect. These data indicate that the long-mysterious requirement for a translation inhibitor (cycloheximide) in TNF $\alpha$ -mediated apoptosis can be explained through lowered cIAP protein amounts. Likewise, lower XIAP levels would promote caspase 3 activation, the latter being observed 2 hours after caspase 8 activation (Fig. 3C). Interestingly, compound **3** has little if any effect on TNF $\alpha$ -induced activation of NF- $\kappa$ B and JNK signaling pathways (fig. S4).

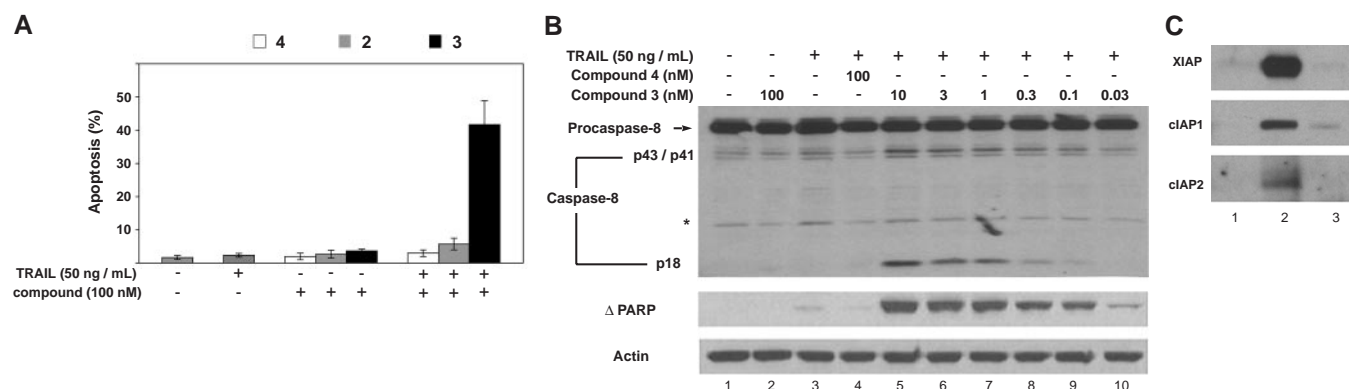


**Fig. 2.** Compound **3** and TRAIL act synergistically to induce apoptosis in cell culture. (A) Human glioblastoma (T98G) cells were cultured in Dulbecco’s minimum essential medium (DMEM) containing fetal calf serum (10%) and treated with TRAIL (50 ng/mL) alone or compound (100 nM) alone for 15 and 19 hours, respectively. When used together, the small molecule was added 4 hours before TRAIL (total incubation time, 19 hours). Cell death (% of total population) was quantified by trypan blue staining. Values represent the average of three independent experiments (error bars indicate 1 standard derivation). (B) Activation of caspase 8 and caspase 3 by **3** in combination with TRAIL. T98G cells were treated with TRAIL (50 ng/ml) alone or **3** (100 nM) alone (for 8 and 12 hours, respectively) or were treated first with various

concentrations of **3** for 4 hours and then with TRAIL for 8 hours. Cell extracts were prepared and subjected to Western blot analysis with the use of antibodies specific for caspase 8 and proteolyzed PARP. Asterisk indicates cross-reactive band. (C) Affinity purification of IAP proteins using a biotinylated form of compound **3** (fig. S2). Biotinylated **3** was immobilized onto streptavidin-conjugated beads and incubated with T98G cell extracts. The recovered beads were boiled, and released proteins were resolved by gel electrophoresis. The gel was probed with antibodies to XIAP, cIAP1 and cIAP2: Lane 1, precipitation using a negative control compound. Lane 2, precipitation using biotinylated **3**. Lane 3, same as lane 2, except the cell extract was treated first with **3** (5  $\mu$ M) for 4 hours.

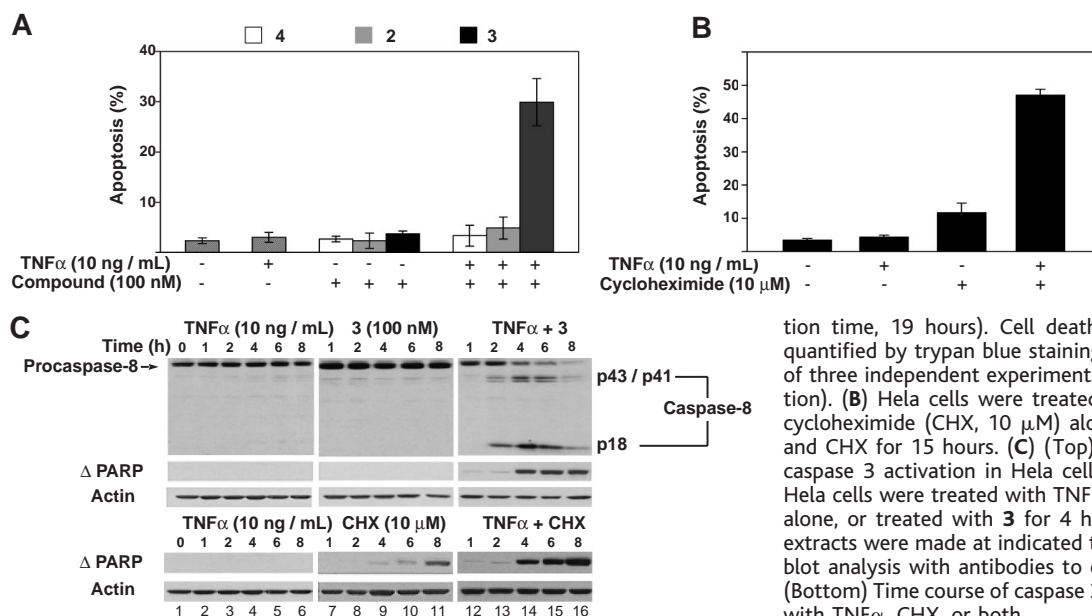


**Fig. 3.** Compound **3** and TNF $\alpha$  act synergistically to induce apoptosis in cell culture. (A) HeLa cells were cultured in DMEM containing fetal calf serum (10%) and treated with TNF $\alpha$  (10 ng/mL) alone or compound (100 nM) alone for 15 and 19 hours, respectively. When used together, the small molecule was added 4 hours before TNF $\alpha$  (total incubation time, 19 hours). Cell death (% of total population) was quantified by trypan blue staining. Values represent the average of three independent experiments (error bars, 1 standard derivation). (B) HeLa cells were treated with TNF $\alpha$  (10 ng/ml) alone, cycloheximide (CHX, 10  $\mu$ M) alone, or a combination of TNF $\alpha$  and CHX for 15 hours. (C) (Top) Time course of caspase 8 and caspase 3 activation in HeLa cells treated with TNF $\alpha$  and/or **3**. HeLa cells were treated with TNF $\alpha$  (10 ng/ml) alone, **3** (100 nM) alone, or treated with **3** for 4 hours and then with TNF $\alpha$ . Cell extracts were made at indicated times and subjected to Western blot analysis with antibodies to caspase 8 or proteolyzed PARP. (Bottom) Time course of caspase 3 activation in HeLa cells treated with TNF $\alpha$ , CHX, or both.

This suggests that the primary role for cIAP-1 and cIAP-2 is to block caspase 8 activation. It also verifies a previous proposal that cIAPs act downstream of NF- $\kappa$ B during its cell survival pathway (25, 26). NF- $\kappa$ B signaling is insufficient to block the onset of apoptosis in the presence of Smac or compound 3. The ability of compound 3 to potentiate apoptosis in TNF $\alpha$ -treated cells, despite NF- $\kappa$ B activation, suggests a strategy for treating inflammatory disease such as rheumatoid arthritis (RA). TNF $\alpha$  functions in RA by inducing secretion of matrix-degrading proteases and multiple inflammatory cytokines and chemokines and increased expression of class I major histocompatibility molecules by synovial fibroblasts (leading to cartilage and bone erosion) and synovial neoangiogenesis (27). Moreover, it stimulates adhesion molecules on the surface of vascular endothelial cells to recruit circulating leukocytes to the endothelium and activates multinucleated osteoclasts to form a seal around bone, where they cause erosion by acidic secretions and protease activity (28). If the original TNF $\alpha$  signal terminated in cell death, it is possible that these downstream events would be avoided.

References and Notes

1. N. A. Thornberry, Y. Lazebnik, *Science* **281**, 1312 (1998).
2. Q. L. Deveraux, J. C. Reed, *Genes Dev.* **13**, 239 (1999).
3. X. Wang, *Genes Dev.* **15**, 2922 (2001).
4. J. Chai *et al.*, *Nature* **406**, 855 (2000).
5. A. G. Uren, M. Pakusch, C. J. Hawkins, K. L. Puls, D. L. Vaux, *Proc. Natl. Acad. Sci. U.S.A.* **93**, 4974 (1996).
6. M. Rothe, M. G. Pan, W. J. Henzel, T. M. Ayres, D. V. Goeddel, *Cell* **83**, 1243 (1995).
7. I. Imoto *et al.*, *Cancer Res.* **61**, 6629 (2001).
8. T. Hasegawa *et al.*, *Blood* **101**, 1164 (2003).
9. M. Krajewska *et al.*, *Clin. Cancer Res.* **9**, 4914 (2003).
10. C. Du, M. Fang, Y. Li, L. Li, X. Wang, *Cell* **102**, 33 (2000).
11. A. M. Verhagen *et al.*, *Cell* **102**, 43 (2000).
12. Single-letter abbreviations for the amino acid residues are as follows: A, Ala; E, Glu; F, Phe; I, Ile; K, Lys; P, Pro; Q, Gln; and V, Val.
13. G. Wu *et al.*, *Nature* **408**, 1008 (2000).
14. Z. Liu *et al.*, *Nature* **408**, 1004 (2000).
15. S. Fulda, W. Wick, M. Weller, K. M. Debatin, *Nat. Med.* **8**, 808 (2002).
16. O. E. Pardo *et al.*, *Mol. Cell. Biol.* **23**, 7600 (2003).
17. L. Yang *et al.*, *Cancer Res.* **63**, 831 (2003).
18. C. R. Arnt, M. V. Chiorean, M. P. Heldebrandt, G. J. Gores, S. H. Kaufmann, *J. Biol. Chem.* **277**, 44236 (2002).
19. This nomenclature refers to the AVPF prototype where the N-terminal L-alanine is position 1 and L-phenylalanine is position 4. Ten surrogates for a proline-phenylalanine dipeptide and 18 variable amino acid residues at position two were combined for a total of 180 compounds.
20. The conversion of 2 to 3 shown in Fig. 1A is an optimized version (29) of an oxidation first observed as a minor competing pathway during Cu<sup>I</sup>-catalyzed cycloadditions of 2 to alkyl azides.
21. M. Mammen, S.-K. Choi, G. M. Whitesides, *Angew. Chem. Int. Ed. Engl.* **37**, 2754 (1998).
22. Y. Huang, R. L. Rich, D. G. Myszk, H. Wu, *J. Biol. Chem.* **278**, 49517 (2003).
23. Under conditions identical to those used in Fig. 1F, neither Smac nor compound 3 block the interaction of XIAP with activated caspases 3. However, both relieve XIAP suppression of caspase 3 activity (fig. S5).

24. Y. Deng, X. Ren, L. Yang, Y. Lin, X. Wu, *Cell* **115**, 61 (2003).
25. C. Y. Wang, M. W. Mayo, R. G. Korneluk, D. V. Goeddel, A. S. Baldwin Jr., *Science* **281**, 1680 (1998).
26. Z. L. Chu *et al.*, *Proc. Natl. Acad. Sci. U.S.A.* **94**, 10057 (1997).
27. D. A. Fox, *Arch. Intern. Med.* **160**, 437 (2000).
28. J. Lam *et al.*, *J. Clin. Invest.* **106**, 1481 (2000).
29. R. Berscheid, F. Vögtle, *Synthesis* **1992**, 58 (1992).
30. We thank O. Guryev for invaluable technical assistance, J. Chen for helpful discussions, N. Williams for preliminary toxicological data, and M. S. Brown and S. L. McKnight for helpful suggestions. Funding provided by a program project grant from the National Cancer

Institute (PO1 CA95471). J.K.D. and P.G.H. are fellows of the Alfred P. Sloan Foundation. P.G.H. acknowledges unrestricted research awards from Eli Lilly, Pfizer, and AstraZeneca. Molecular interaction data have been deposited in the Biomolecular Interaction Network Database with accession codes 150999 to 151001.

Supporting Online Material

www.sciencemag.org/cgi/content/full/305/5689/1471/DC1

Figs. S1 to S6

23 March 2004; accepted 15 June 2004

# The Emergence of Competition Between Model Protocells

Irene A. Chen,<sup>1,2</sup> Richard W. Roberts,<sup>3</sup> Jack W. Szostak<sup>1\*</sup>

The transition from independent molecular entities to cellular structures with integrated behaviors was a crucial aspect of the origin of life. We show that simple physical principles can mediate a coordinated interaction between genome and compartment boundary, independent of any genomic functions beyond self-replication. RNA, encapsulated in fatty acid vesicles, exerts an osmotic pressure on the vesicle membrane that drives the uptake of additional membrane components, leading to membrane growth at the expense of relaxed vesicles, which shrink. Thus, more efficient RNA replication could cause faster cell growth, leading to the emergence of Darwinian evolution at the cellular level.

A simple model of a primitive cell involves a self-replicating genome, such as an RNA polymerase ribozyme (a “replicase”), and an encapsulating membrane that can grow and divide (1) (supporting online text). Genomic influence over vesicle growth has been assumed to require a second RNA function, such as a ribozyme that would synthesize membrane components (2). Although such molecules presumably evolved at some point, we wondered whether the transition to a unified cell might have been facilitated by simpler physical mechanisms for coupling genomic properties and membrane behavior.

We sought to detect the emergence of an adaptive cellular-level trait based on the physical properties of a model prebiotic vesicle system containing encapsulated nucleic acids. Counterions associated with RNA encapsulated by a semipermeable membrane exert osmotic pressure on the membrane, which is counterbalanced by membrane tension. RNA replication would convert freely diffusing nucleic acid monomers into large impermeable macromolecules, increasing the concentration of trapped counterions. The re-

sulting increase in osmotic pressure and membrane tension would create a driving force for an increase in membrane area, thereby coupling RNA replication to membrane growth (supporting online text).

We tested whether fatty acid vesicles (3–5) (supporting online text) osmotically stressed by encapsulated contents would increase in membrane area at the expense of unstressed vesicles. An initial concern was that fatty acid membranes might be too structurally weak to maintain a substantial osmotic gradient. We therefore determined the maximum sustainable membrane tension of oleate (C18:1) vesicles under osmotic stress. Oleate vesicles (100-nm diameter) encapsulating 1 M sucrose were diluted into hypotonic buffers (6). Applied gradients  $\geq 0.7$  M caused transient membrane rupture and release of solutes, detectable by size-exclusion chromatography, followed by membrane resealing at a maximal sustainable membrane tension ( $\tau^*_{\text{oleate}}$ ). After accounting for vesicle swelling from the extruded nonspherical shape to a spherical shape (7, 8) and the partial loss of encapsulated solutes, we estimate that  $\tau^*_{\text{oleate}}$  is 10 dyn/cm, or 4 atm. A similar experiment with 100 nm POPC (1-palmitoyl-2-oleoyl-*sn*-glycero-3-phosphocholine) vesicles showed that  $\tau^*_{\text{POPC}}$  is 25 dyn/cm (supporting online text). These measurements fall within the range previously reported for phospholipid membranes (3 to 40 dyn/cm) (9–11). Thus, fatty acids, though chemically simple, can indeed form surprisingly strong membranes under osmotic stress.

<sup>1</sup>Department of Genetics, Harvard Medical School, and Howard Hughes Medical Institute, Department of Molecular Biology, Massachusetts General Hospital, Boston, MA 02114, USA. <sup>2</sup>Program in Biophysics, Harvard University, Cambridge, MA 02138, USA. <sup>3</sup>Division of Chemistry and Chemical Engineering, California Institute of Technology, Pasadena, CA 91125, USA.

\*To whom correspondence may be addressed. E-mail: szostak@molbio.mgh.harvard.edu